

DERIVATION OF SOLAR FLARE CELLULAR AUTOMATA MODELS FROM A SUBSET OF THE MAGNETOHYDRODYNAMIC EQUATIONS

D. VASSILIADIS,¹ A. ANASTASIADIS,² M. GEORGIOULIS,² AND L. VLAHOS²

Received 1998 July 13; accepted 1998 September 28; published 1998 November 10

ABSTRACT

Cellular automata (CA) models account for the power-law distributions found for solar flare hard X-ray observations, but their physics has been unclear. We examine four of these models and show that their criteria and magnetic field distribution rules can be derived by discretizing the MHD diffusion equation as obtained from a simplified Ohm’s law. Identifying the discrete MHD with the CA models leads to an expression for the resistivity as a function of the current on the flux tube boundary, as may be expected from current-driven instabilities. Anisotropic CA models correspond to a nonlinear resistivity $\eta(\mathbf{J})$, while isotropic ones are associated with hyperresistivity $\eta(\nabla^2 \mathbf{J})$. The discrete equations satisfy the necessary conditions for self-organized criticality (Lu): there is local conservation of a field (magnetic flux), while the nonlinear resistivity provides a rapid dissipation and relaxation mechanism. The approach justifies many features of the CA models that were originally based on intuition.

Subject headings: chaos — diffusion — MHD — Sun: flares — Sun: magnetic fields — turbulence

1. INTRODUCTION

Cellular automata (CA) models produce power-law distributions of events (Lu & Hamilton 1991, hereafter LH91; Lu et al. 1993, hereafter L93; Vlahos et al. 1995, hereafter V95; Georgoulis & Vlahos 1996, hereafter GV96; Georgoulis & Vlahos 1998) similar to those found observationally for hard X-ray (HXR) flare parameters such as total released energy, peak luminosity, and flare duration (Dennis 1985; Lin et al. 1984; Kucera et al. 1997; Crosby et al. 1998; Georgoulis, Vilmer, & Crosby 1998). It will be shown below that many of the intuitive choices for the model rules and dynamics have a simple physical justification.

The automata are systems discrete in space and time with deterministic evolution rules that prescribe how to transport a field quantity from one “cell” of the automaton to the next. The field is usually called the magnetic field, although the rules are not derived from physical laws. At every iteration a random amount of field is added to a randomly chosen cell, simulating the addition of field due to either shuffling of the field lines or emerging flux. When the field in a cell exceeds a threshold value, the cell becomes unstable and the excess field is distributed to its nearest neighbors. The reconfiguration can trigger secondary instabilities in neighboring cells; after all adjacent cells have become stable again, the “avalanche” ends. Avalanches may extend to a volume comparable to the system size until they reach the absorbing boundaries. Asymptotically the distribution of avalanche amplitude, duration, and time-integrated energy reaches a power-law form apparently independently of the details of the automaton rules. The numerical values of the power laws are similar to the observed ones for HXR flares. The phenomenon of developing such a scale-invariant state is called self-organized criticality (SOC) (Bak, Tang, & Wiesenfeld 1987; Hwa & Kardar 1992) and has been related to the marginal stable states in a plasma (Diamond & Hahn 1995). SOC was originally shown to appear in discrete

systems, but Lu (1995) discusses the conditions necessary for a continuous system to reach such a state.

Here we derive several of the CA models from a subset of MHD equations, showing the physics that can be attributed to the CA rules. A companion paper by Isliker et al. (1998) starts from the LH91 model and derives a corresponding partial differential equation in the continuum limit.

2. MHD EQUATIONS AND DISCRETIZATION

Since the cellular automata model the transport of magnetic field, the starting point is Faraday’s law, $(\partial \mathbf{B} / \partial t) = -\nabla \times \mathbf{E}$. A simplified Ohm’s law, $\mathbf{E} = \eta \mathbf{J} - \mathbf{v} \times \mathbf{B}$, where η is the resistivity, gives the induction equation

$$\frac{\partial \mathbf{B}}{\partial t} = -\nabla \times (\eta \mathbf{J}) + \nabla (\mathbf{v} \times \mathbf{B}), \quad (1)$$

$$= -\nabla \times (\eta \mathbf{J}) + \mathbf{S}(\mathbf{x}; t), \quad (2)$$

where $\mathbf{J} = (1/\mu_0) \nabla \times \mathbf{B}$. In equation (2) the $\mathbf{v} \times \mathbf{B}$ term has been replaced by a more general source term, $\mathbf{S}(\mathbf{x}, t)$, whose physical sources are the velocity shear and, in addition, emerging flux. The loading is of low amplitude and is slow compared to the timescale for magnetic field diffusion, $\mu_0 l^2 / \eta$, where l is the smallest size of the system (to be identified with the cell size below) (see also LH91). Equation (2) is similar to a CA model if we note that the threshold criteria and distribution rules of CA models resemble low-order discrete temporal and spatial derivatives (Vassiliadis et al. 1996).

The configuration we choose is that of a strongly magnetized plasma with a purely axial field, $\mathbf{B} = B(x, y; t) \hat{\mathbf{z}}$, where we examine the perpendicular field transport on the (x, y) -plane. The plane is discretized using a square lattice (Fig. 1) of cell size l . Hence the flux tube cross section is a set of adjacent cells sharing the same field magnitude; conversely a cell can constitute an “elementary” flux tube. (For a simulation of a part of a solar active region, for example, each cell would represent the horizontal cross section of a coronal loop, and its size would correspond to a physical dimension of approximately 100 km.) The value of l is not expected to change the self-similar nature of the resulting event distributions but,

¹ NASA/GSFC/USRA, Code 692, Greenbelt, MD 20771; vassi@lepgst.gsfc.nasa.gov.

² Section of Astrophysics, Astronomy, and Mechanics, Department of Physics, University of Thessaloniki, 54006 Thessaloniki, Greece; anastasi@astro.auth.gr, georgoul@astro.auth.gr, vlahos@astro.auth.gr.

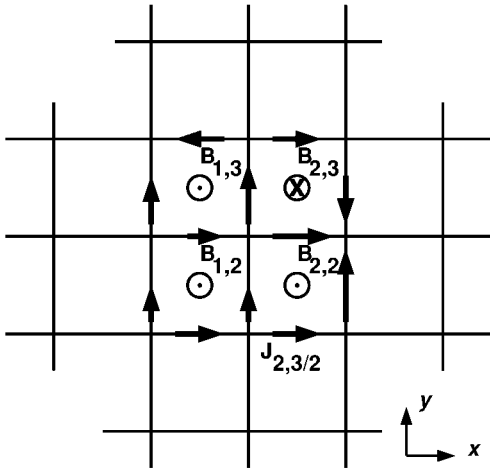


FIG. 1.—Two-dimensional configuration for the discrete MHD equations. Flux tubes (cells) form a lattice on the (x, y) -plane, and each contains a purely axial \mathbf{B} -field, while currents \mathbf{J} flow on the flux tube boundaries (eq. [3]).

rather, only the lower end of the energy and duration range. From here on we use the terms “flux tube” and “cell” interchangeably.

We discretize Ampere’s law by having the currents flow on the flux tube boundary, rather than within the cell volume. The boundary between cells (x, y) and $(x + 1, y)$ is denoted by $(x + 1/2, y)$ so Ampere’s law becomes

$$\begin{aligned} J_{x+1/2,y} &= \frac{1}{\mu_0} (\nabla \times \mathbf{B}) \cdot \hat{y} \\ &= \frac{1}{\mu_0} (B_{x,y} - B_{x+1,y}). \end{aligned} \quad (3)$$

Similarly there is a current on the boundaries in the x -direction, $J_{x,y+1/2}$. This discretization, similar to a staggered-grid scheme, is space-centered for both \mathbf{B} and \mathbf{J} and ensures that $\nabla \mathbf{J} = 0$ at the lattice points. It does not represent field-aligned currents. Another useful quantity, the Laplacian $\mathbf{L}_{x,y} = \nabla^2 \mathbf{B} = -\mu_0 \nabla \times \mathbf{J}$, is written

$$\mathbf{L}_{x,y} = \mu_0 (J_{x-1/2,y} - J_{x+1/2,y} + J_{x,y-1/2} - J_{x,y+1/2}) \hat{z}, \quad (4)$$

and, like \mathbf{B} , it is associated with the cell “volume” rather than the cell boundary.

For the resistivity η there is the choice of considering it as a property of the flux tube volume or of the boundary between two flux tubes. From the configuration’s symmetry and in order for η to couple to and depend on \mathbf{J} , we define η to be a property of the boundary and denote it by $\eta_{x+1/2,y}$. This defines the electric field along the boundary, $E_{x+1/2,y} = (\eta J)_{x+1/2,y}$. The form of η as a function of the local \mathbf{B} configuration will be obtained from comparison with the CA rules. In order for the model to reproduce flare statistics with realistic timescales, we expect that an anomalous resistivity will be needed; a classical η gives diffusion timescales that are too long compared to observations.

Equation (2) is discretized as

$$\begin{aligned} B_{x,y}(t+1) &= B_{x,y} - \frac{\Delta t}{\Delta x} [(\eta J)_{x+1/2,y} - (\eta J)_{x-1/2,y} \\ &\quad - (\eta J)_{x,y+1/2} + (\eta J)_{x,y-1/2}] + S_{x,y}(t), \end{aligned} \quad (5)$$

$$\begin{aligned} B_{x,y}(t+1) &= B_{x,y} + \frac{\Delta t}{\mu_0 \Delta x^2} [\eta_{x+1/2,y} (B_{x+1,y} - B_{x,y}) \\ &\quad - \eta_{x-1/2,y} (B_{x,y} - B_{x-1,y}) \\ &\quad + \eta_{x,y+1/2} (B_{x,y+1} - B_{x,y}) \\ &\quad - \eta_{x,y-1/2} (B_{x,y} - B_{x,y-1})] + S_{x,y}(t), \end{aligned} \quad (6)$$

where all the quantities on the right are evaluated at time t , and where we have omitted the unit direction vectors (all parallel to \hat{z}). In the following, we set the length and timescales, $\Delta x (= l)$ and Δt , equal to 1, while more generally their values can be absorbed in a rescaled η . If the resistivity depends on \mathbf{J} and other boundary variables, rather than \mathbf{B} and cell variables, the transported flux across a boundary, ηJ , is equal and opposite for the donor and the receptor cell, and therefore the discretization (6) automatically conserves B_z (except for the new field added by the source). Conservation of a field variable is a necessary condition for SOC (Lu 1995; Hwa & Kardar 1992).

The energy lost in a flux tube that undergoes an elementary avalanche is the energy density $(1/2\mu) [B_{x,y}^2(t+1) - B_{x,y}^2(t)]$ integrated over the flux tube cross section (similar to the CA models), while the energy dissipation on a boundary is $(\eta J^2)_{x+1/2,y} \Delta t$.

The discrete scheme (eq. [7]) is a coupled map lattice (CML). Both CA and CML are discrete in space and time, but CA variables are integer, whereas CML variables are real or complex fields (see, e.g., Bunimovich 1997). The flare “CA” models are, strictly speaking, also CMLs.

3. DERIVATION OF THE CA MODEL RULES

3.1. Linear Diffusion

If η is constant everywhere, equation (2) gives the linear diffusion equation written as

$$\begin{aligned} B_{x,y}(t+1) &= B_{x,y} + \frac{\eta}{\mu_0} (B_{x+1,y} - 2B_{x,y} + B_{x-1,y}) \\ &\quad + \frac{\eta}{\mu_0} (B_{x,y+1} - 2B_{x,y} + B_{x,y-1}). \end{aligned} \quad (7)$$

The discrete MHD scheme does not resolve timescales shorter than t_{diff} but gives the solution of the continuous MHD equations at longer timescales (Islaker et al. 1998).

3.2. Anisotropic Models

If η varies with space and time, a more complex dynamics is obtained. In order to reproduce CA rules, η depends on the local \mathbf{J} configuration in such a way that when new flux $\delta \mathbf{B}$ is added to a cell, it does not diffuse until the conditions on one of the flux tube boundaries exceed a critical threshold. Then diffusion takes place only across that boundary without affecting η at the other boundaries. This type of diffusion may be associated with a kink or interchange MHD instability and

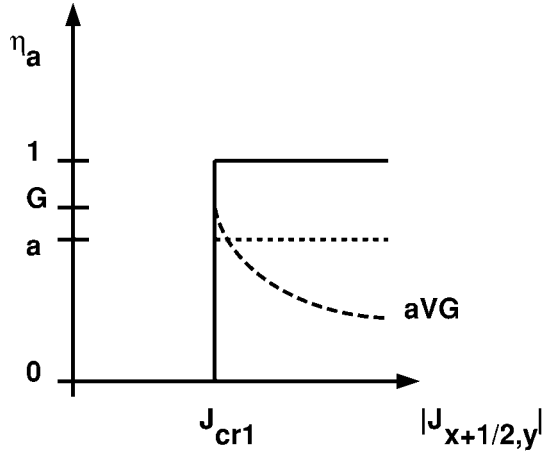


FIG. 2.—Anisotropic models. The resistivity η is a function of current $J_{x+1/2,y}$ along one of the cell boundaries (eq. [8]). When the threshold is exceeded, the excess field $\mu_0 J_{x+1/2,y}$ can be redistributed as one of the following: all at once (eq. [9]) (solid line); only at a fraction, $\eta_a J_{x+1/2,y}$, $\eta_a \leq 1$ (dotted line); or at a fixed amount, proportional to the critical current J_{cr1} . A discrete MHD model with the latter resistivity is equivalent to the aVG model.

can be triggered by shuffling the photospheric footpoints of flux tubes (the motion itself is not modeled since $v = 0$). With this resistivity we recover the rules of the anisotropic CA models of V95 and GV96 (hereafter referred to as aVG), which produce low-amplitude events, or model “nanoflares.” The instability criteria are easier to satisfy than the isotropic resistivity (see § 3.3, below) and may represent localized jetting and/or heating due to reconnection at the flux tube boundary.

In the discrete MHD model (6) the η on one of the flux tube’s boundaries turns on when a threshold J_{cr1} is exceeded. This can be simply a piecewise-constant function (Fig. 2, solid line):

$$\eta_{x+1/2,y} = \eta_a \Theta(|J_{x+1/2,y}| - J_{cr1}), \quad (8)$$

with Θ being the step function. The field transferred is $\eta_a J_{x+1/2,y}$, where $\eta_a \leq 1$ with the equality corresponding to removal of all excess field. Instead of fixing the ratio between excess and transferred field, one can fix the amount transferred, as is done in the aVG model, which transfers an amount of field proportional to J_{cr1} . In order to obtain η_a we equate the expression for the transferred field from the discrete MHD model to that of the CA rules:

$$\eta_a = G_a \frac{J_{cr1}}{J_{x+1/2,y}}, \quad (9)$$

where the geometric factor $G_a = nn/[r(nn + 1)]$ depends on the dimension and type of lattice, nn is the number of nearest neighbor flux tubes, and $r \leq nn$ is the number of unstable nearest neighbors. (We consider only first-order nearest neighbors, which is called Criterion I in the aVG model). In summary the discrete MHD model reproduces the anisotropic CA distribution rules and therefore will produce the same dynamics, including SOC, if it is driven with the same source.

3.3. Isotropic Models

Here the criterion for \mathbf{B} -field transport depends on the difference between the flux tube and the average of its neighbors,

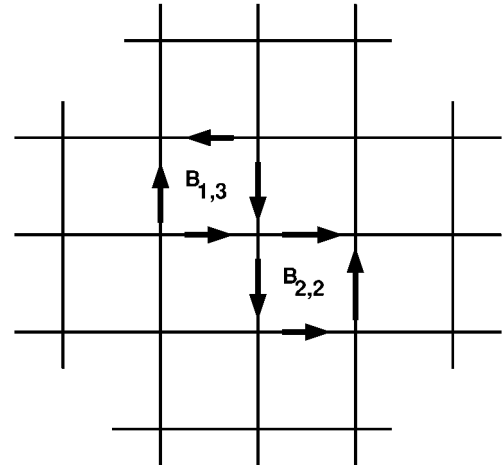


FIG. 3.—The Laplacian $L = \nabla^2 \mathbf{B} = -\mu_0 \nabla \times \mathbf{J}$ in a flux tube is calculated from the current integrated around the flux tube boundary (net current). Cells of zero and nonzero $L_{x,y}$ are shown ($B_{1,3}$ and $B_{2,2}$, respectively).

$B_{x,y} - (1/nn) \sum_{nn} B_{x,y;nn}$ (LH91; L93; V95; GV96), where $B_{x,y;nn}$ is a nearest neighbor of $B_{x,y}$. The difference can be rewritten in terms of the Laplacian (4), as $(1/nn \cdot \mu_0) L_{x,y}$, and since $L_{x,y}$ is proportional to the net current flowing around the boundary (Fig. 3), the relevant physical quantity is the average net current $J_{x,y;av} = (1/nn \cdot \mu_0) \nabla \times L_{x,y}$, obtained by subtracting the average currents on adjacent flux tubes.

In the discrete MHD model the resistivity increases when the average net current of the cell exceeds a threshold. This is still a local instability since it depends on conditions of a single flux tube, the most elementary structure of the system. However, since it is the average current that exceeds the threshold, the instability can be considered to spread to the boundaries of the flux tube “instantaneously,” i.e., faster than Δt . The electric field $\mathbf{E} = \eta \mathbf{J}$ with $\eta = f(\nabla \times L)$ can be rewritten in terms of $\nabla^2 \mathbf{J}$ (since $\nabla \mathbf{J} = 0$) and can be interpreted as a hyperresistivity (Biskamp 1993) effect. Hyperresistivity is associated with a fast electron response. The trigger of a high-speed instability can be a large δB -deposition on a single cell representing intense photospheric emerging flux. In CA models, isotropic avalanches triggered by large δB are events significantly larger in size and longer in duration than anisotropic avalanches (Vlahos et al. 1995).

For the resistivity of the isotropic model we have (see Fig. 4)

$$\eta_{x+1/2,y} = \eta_i \Theta(|J_{x+1/2,y;av}| - J_{cr2}). \quad (10)$$

For the isotropic VG model (V95; GV96) (hereafter iVG) the field transferred across the boundary is fixed, $G_i J_{cr2}$, so the amplitude is

$$\eta_i = \eta_{iVG} = G_i \frac{J_{cr2}}{J}, \quad (11)$$

with a geometric factor $G_i = 1/(nn + 1)$, and with J now denoting the magnitude of \mathbf{J} on the boundary (Fig. 4, dotted line). Similarly to the aVG model, equation (11) places an upper limit to the transported field in one time step, which results in prolonging the duration of avalanches, especially those due to large $|\delta \mathbf{B}|$.

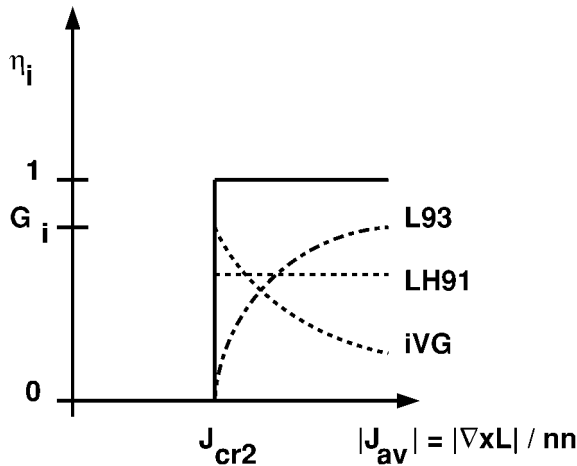


FIG. 4.—Isotropic models. As eq. (10) shows, the resistivity depends on the average net current around the flux tube: $J_{x,y;av} = (1/mn) \nabla \times \mathbf{L}_{x,y}$. A fraction of the excess field is redistributed in the following ways: η decreases as $J_{x,y;av}$ increases (iVG model, *dotted line*); is independent of current so that all the excess \mathbf{B} is redistributed (LH91 model, *dashed line*); or increases with $J_{x,y;av}$ (L93 model, *dash-dotted line*), which extends the duration of large avalanches.

The two earlier isotropic models are slightly different. The original CA model (LH91) transfers all the excess field in one step, and after the avalanche is over, $J_{x+1/2,y;av}$ is zero, so the corresponding η is $\eta_i = \eta_{LH91} = G_i (J_{x+1/2,y;av}/J)$. In the special case when $J = J_{x+1/2,y;av}$, η is piecewise constant (Fig. 4). Finally in the L93 model, only part of the excess current, $J_{x+1/2,y;av} - J_{cr2}$, is transported so that $\eta_i = \eta_{L93} = G_i [(J_{x+1/2,y;av} - J_{cr2})/J]$.

4. SUMMARY AND DISCUSSION

The discrete MHD model reproduces the rules, and therefore the dynamics, of CA (actually CML) models for solar flare statistics and shows that they represent a diffusion of \mathbf{B} based on a nonlinear current-dependent resistivity η . The discretization scheme conserves local flux, and the resistivity produces a rapid field relaxation and energy dissipation, all of which are necessary properties for SOC (Hwa & Kardar 1992; Lu 1995). The discrete MHD model has a computational cycle consisting of (eqs. [6], [3], and [8]–[10]) similar to the integration of the standard MHD simulation. Loading can take place at every time step without interruptions during avalanches. This type of loading produces “running avalanches” (Hwa & Kardar 1992) and is more realistic than the stop-and-go loading of flare CA models. The form of the effective resistivity $\eta(\mathbf{J})$ can be obtained from physical considerations, e.g., anomalous transport coefficients (Papadopoulos 1985), and in addition can be scaled appropriately to match the observed power-law distributions.

Currently we are investigating a continuously loaded (in the manner of Hwa & Kardar 1992) discrete-MHD scheme. Using this MHD diffusion simulation, it will be possible to extend the CA/CML models further and examine under what conditions SOC is preserved; to that end additional variables can be included, such as the velocity and electric fields.

We thank H. Isliker, M. Aschwanden, G. Holman, M. Pet-saga, and G. Vetoulis for useful discussions. We appreciate the referee’s comments, which led to an improvement of the presentation. The work of Anastasiadis, Vassiliadis, and Vlahos is part of a visiting scientist program (PENED) of the General Secretariat for Research and Technology of Greece. Georgoulis was supported by the Government Scholarship Foundation (IKY) of Greece.

REFERENCES

- Bak, P., Tang, C., & Wiesenfeld, K. 1987, *Phys. Rev. Lett.*, 59, 381
 Biskamp, D. 1993, *Nonlinear Magnetohydrodynamics* (Cambridge: Cambridge Univ. Press)
 Bunimovich, L. A. 1997, *Physica D*, 103, 1
 Crosby, N. B., Vilmer, N., Lund, N., & Sunyaev, R. 1998, *A&A*, 334, 299
 Dennis, B. R. 1985, *Sol. Phys.*, 100, 465
 Diamond, P. H., & Hahm, T. S. 1995, *Phys. Plasmas*, 2, 3640
 Georgoulis, M. K., & Vlahos, L. 1996, *ApJ*, 469, L135 (GV96)
 ———. 1998, *A&A*, 336, 721
 Georgoulis, M. K., Vilmer, N., & Crosby, N. B. 1998, *A&A*, submitted
 Hwa, T., & Kardar, M. 1992, *Phys. Rev. A*, 45, 7002
 Isliker, H., Anastasiadis, A., Vassiliadis, D., & Vlahos, L. 1998, *A&A*, 335, 1085
 Kucera, T. A., Dennis, B. R., Schwartz, R. A., & Shaw, D. 1997, *ApJ*, 475, 338
 Lin, R. P., Schwartz, R. A., Kane, S. R., Pelling, R. M., & Hurley, K. C. 1984, *ApJ*, 283, 421
 Lu, E. T. 1995, *Phys. Rev. Lett.*, 74, 2511
 Lu, E. T., & Hamilton, R. J. 1991, *ApJ*, 380, L89 (LH91)
 Lu, E. T., Hamilton, R. J., McTiernan, J. M., & Bromund, K. R. 1993, *ApJ*, 412, 841 (L93)
 Papadopoulos, K. 1985, in *Collisionless Shocks in the Heliosphere: A Tutorial Review*, ed. R. G. Stone & B. T. Tsurutani (Washington, DC: AGU), 59
 Vassiliadis, D., Vlahos, L., Georgoulis, M., & Kluiving, R. 1996, unpublished
 Vlahos, L., Georgoulis, M., Kluiving, R., & Paschos, P. 1995, *A&A*, 299, 897 (V95)